Delta Wing in Waves

Computational Fluid Dynamics 5 - Assignment 2

THE UNIVERSITY
of EDINBURGH

Pawel Safuryn

16th December 2016

Course organisers:
Prof David Ingram
Dr Ignazio Maria Viola

Abstract

Delta wings are considered as a suitable submerged hydrofoil for a small marine vehicle due to their ability to generate lift at large angles of attack and maintaining it at a relatively steady level when the angle varies. Forces and flow over a slender delta wing are analysed for the conditions of $Re_c = 5 \times 10^4$, $Fr = 0.5048$ and angle of attack $\alpha = 30°$. Presence of head waves is also considered. An unsteady vortex structure was observed at the suction surface of the hydrofoil. It was identified to be the major source of lift generated at high angles of attack. A vortex breakdown was also found to occur at a distance of around 75% of the chord. No reattachment close to the wing midplane was present, which agreed with literature. The estimations of hydrodynamic lift and drag coefficients are $C_L = 1.189 \pm 0.012$ and $C_D = 0.644 \pm 0.023$ at local minima and $C_L = 1.297 \pm 0.012$ and $C_D = 0.698 \pm 0.023$ at local maxima. The information obtained from the simulations can be used to predict maximum payload or power consumption, and make design decisions.

1 Introduction

Delta wings allow for generation of lift forces at very large angles of attack, where conventional high-aspect-ratio wings would stall. Moreover, their shape causes the force variations to be small when the angle of attack is changing in time. For those reasons, delta wings are considered as a suitable submerged hydrofoil for a small marine vehicle.

The goal of the assignment is to model a submerged delta wing to estimate the hydrodynamic lift and drag coefficients and the flow field around the wing when sailing in head waves. Such information could be used by a design company to predict maximum payload or power consumption, and make decisions on how to connect the hydrofoil to the vessel. The project considers the flow conditions of $Re_c = 5 \times 10^4$, $Fr = 0.5048$ and angle of attack $\alpha = 30°$. The numerical model and analysis of the flow solution are presented in this report.

2 Method

2.1 Main assumptions

The three-dimensional effects of flow around a delta wing are significant for its ability to generate lift at high angles of attack. Therefore, a 3D numerical model was used in the project. Also, due to the nature of the problem (oscillating head waves), a time-dependent analysis was conducted. Such approach is further verified by the existence of periodic vortex shedding predicted by literature [1].

The effect of head waves was modelled using custom user functions which described the theoretical wave velocity and pressure fields varying in space and time. Despite the waves being gravity driven in a real scenario, such approach allowed for neglecting the gravity effects in the simulation. This was further verified by obtaining a small value for the theoretical difference between hydrostatic pressures across the delta wing. For those reasons and a low expected time variation in pressure, water was also treated as an incompressible fluid. Finally, the turbulence length scale l was estimated from the hydraulic diameter d_h using equation: $l = 0.038 d_h$. A medium turbulence case was assumed with intensity of $I = 0.01$.

The thickness of the delta wing analysed was chosen to be 4% of the chord as used by Gursul [2]. Also, the leading edge was modelled to be semi-circular as, according to Gursul, flow features are strongly affected by the leading edge shape and round edges provide the most realistic configurations. With a sweep angle of $\Lambda = 64.84°$, the hydrofoil modelled can be considered a slender wing [2, 3].

The wave and fluid properties and dimensions of the delta wing were calculated basing on the flow conditions given in the project instructions and are presented in Table 1.

Wave properties		**Fluid and flow properties**		**Delta wing properties**	
Length (λ)	1 m	Freestream speed (U)	0.5 m/s	Root chord (c)	0.1 m
Height (H)	0.01 m	Density (ρ)	1000 kg/m^3	Thickness (t)	0.004 m
Period (T)	0.8 s	Viscosity (μ)	1×10^{-3} Pa·s	Angle of attack (α)	30°
Number (q)	6.28 rad/m	Turb. intensity (I)	0.01	Sweep angle (Λ)	64.84°
Frequency (ω)	7.85 rad/s	Turb. length scale (l)	0.01824 m	Apex depth (z_0)	0.2 m
Celerity (C)	1.25 m/s				

Table 1: Wave, flow and delta wing properties used in the numerical model.

2.2 Domain and grid

The delta wing was positioned at an angle of 30° in a cuboid domain as shown in Figure 1. The two inlets at the top and front faces were defined using a custom vector field function

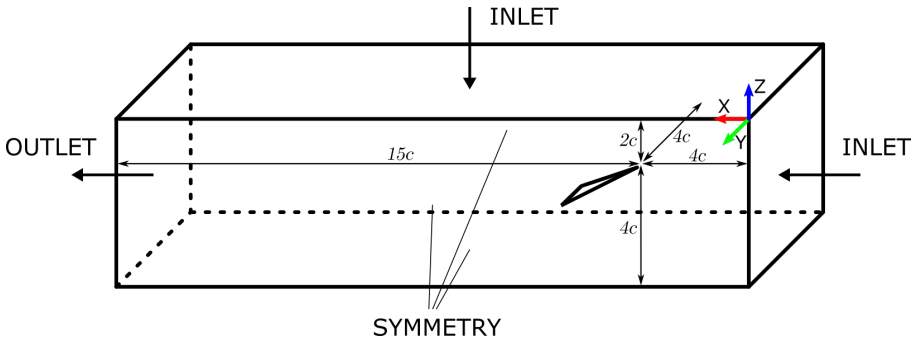

(a)

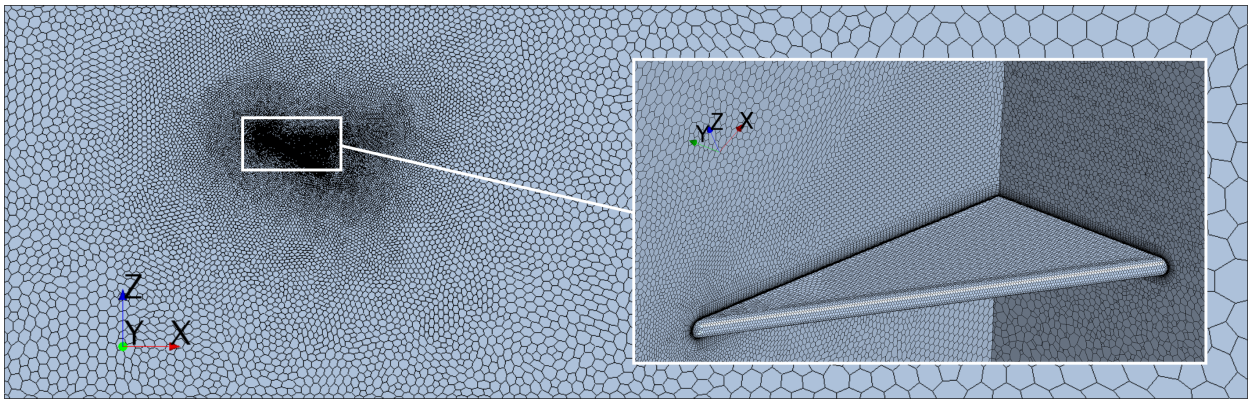

(b)

Figure 1: (a) Domain used in the simulation. (b) Computational mesh for the delta wing.

describing velocities relative to the delta wing (both due to head waves and freestream). The outlet at the back face used a custom scalar field function to describe the pressure caused by the head waves. In terms of backflow specification, the flow direction was extrapolated from the interior of the domain. Same functions were used to initialise the velocities and pressures within the domain. They are given by:

$$\vec{u}(x,y,z,t) = \left[\omega\frac{H}{2}\sin(qx-\omega t)\mathrm{e}^{qz} + 0.5 \quad 0 \quad -\omega\frac{H}{2}\cos(qx-\omega t)\mathrm{e}^{qz}\right] \tag{1}$$

$$P(x,y,z,t) = -\rho\frac{\omega^2}{q}\frac{H}{2}\sin(qx-\omega t)\mathrm{e}^{qz} \tag{2}$$

The pressure outlet was placed far away from the delta wing to ensure it has little effect on the wake formation and that the effect of "flattening waves" is negligible. Fifteen chord lengths was deemed a suitable distance basing on the previous assignment and the work of Collie [4]. The other far-field boundaries (bottom and one side) used symmetry planes and were located four chord lengths away from the delta wing, which was again considered sufficient basing on the distances used by Gordnier [1]. Symmetry condition was also imposed along the midplane of the wing to greatly reduce the computational effort. This was reasonable as initial and boundary conditions, and geometry were all symmetric and symmetric flow pattern was expected. No-slip condition was chosen at the wing surfaces.

A polyhedral mesh with prism layer and surface remesher modules were used to produce the grid for the simulation. Polyhedral mesh was chosen due to its stability, easier setup and expected variations in flow direction over the wing. Volume growing polyhedrons were implemented to grow the size of the cells from the wing towards the faces of the cuboid. Moreover, additional refinements in the wake region were performed using a semi-conical shape with cross-sectional area increasing from the apex of the hydrofoil towards its trailing edge. The detailed diagram of the grid can be seen in Figure 1b. Characteristics of the mesh

were defined in terms of the base size which was varied to produce three grid resolutions and conduct the grid uncertainty study. Focus was also placed on achieving a high quality prism layer on the wing surfaces. The thickness of the first prism layer was set to produce a $y^+ \approx 1$ to resolve the viscous sublayer successfully.

2.3 Equations solved and discretisation

A value of $y^+ \approx 1$ was needed as the k-ω Shear Stress Transport (SST) turbulence model with low y^+ treatment was used in the simulations. A turbulent model was used as, according to Gursul [2], the shear layer reattachment zones can be associated with turbulence activity. The k-ω SST solves the continuity equation and Reynolds-averaged Navier-Stokes (RANS) equations which, for incompressible flow, can be written in Einstein notation as:

$$\rho\left(\frac{\partial\langle u_i\rangle}{\partial t} + \langle u_j\rangle\frac{\partial\langle u_i\rangle}{\partial x_j}\right) = \frac{\partial\langle p\rangle}{\partial x_i} + \frac{\partial}{\partial x_j}\left(\mu\frac{\partial\langle u_i\rangle}{\partial x_j} - \langle\rho u_j' u_i'\rangle\right) \tag{3}$$

The turbulence model uses Boussinesq assumption to represent the Reynolds stresses as:

$$-\langle\rho u_j' u_i'\rangle = \mu_t\left(\frac{\partial\langle u_i\rangle}{\partial x_j} + \frac{\partial\langle u_j\rangle}{\partial x_i}\right) - \frac{2}{3}\rho k\delta_{ij} \tag{4}$$

and provides equations of turbulent kinetic energy k and the specific turbulence dissipation ω to calculate the turbulent viscosity μ_t. Finite Volume discretisation scheme was used in the simulations performed using Star-CCM+ software.

Although less accurate, first order time discretisation was used to ensure reasonable simulation times for given grid sizes. A base time step of 0.02 s was used which was deemed enough to resolve the oscillations of velocities and angle of attack due to the wave period of 0.8 s. This time step was then doubled and halved to conduct time step uncertainty study. It has also been observed by Gordnier [1] that small-scale vortices can be periodically shed from the leading edge with a frequency described by a Strouhal number of $St \approx 10$. This corresponded to a frequency of 50 Hz in conditions analysed in this project. In order to attempt to resolve this vortex shedding, a simulation with a time step of 0.001 s was also run. Only 0.8 s (wave period) of physical time was simulated in this case due to the computational effort required.

3 Results and discussion

Vortex structures were observed in the flow over the delta wing, as expected from literature [1, 2, 3]. The analysis confirmed that the vortices created in the flow are the main reason for the ability of the delta wing to generate lift at high angles of attack. An overview of results obtained is presented in Figure 2. From the streamlines shown, both primary and secondary vortices can be distinguished. Moreover, the pressure distribution on the suction surface of the wing shows a clear correlation with the vortical structures. Parts of the upper surface directly below the vortices have significantly lower pressures, which contribute to higher lift.

Figure 2b also shows the values of coefficients of lift C_L and drag C_D developing in time. A plot of the theoretical change of angle of attack $\alpha = \alpha(t)$ due to the head waves is also plotted on top. It was calculated at the apex of the delta wing ($x = 0.4$ m, $y = 0$ m, $z = -0.2$ m). Lift and drag coefficients are observed to increase as the angle of attack increases, which is expected for the values of Λ and averaged α used in the simulation [2]. However, a small difference in phase is observed, which is due to the variation of local angle of attack and local freestream speed at different points around the wing surface.

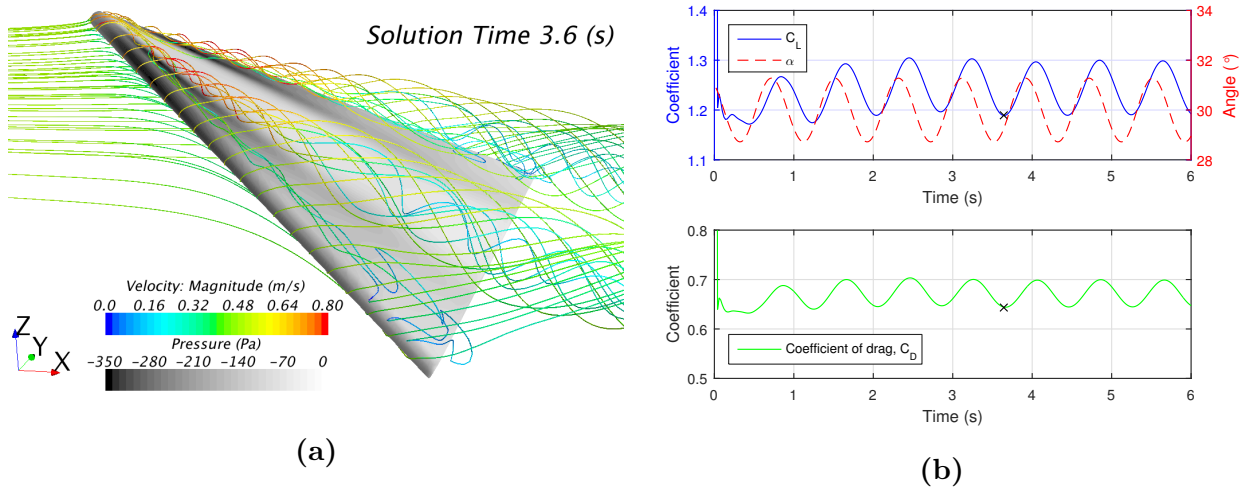

(a) (b)

Figure 2: (a) Flow pattern around the delta wing and (b) C_L and C_D results with angle of attack plot.

Furthermore, the variation of coefficients with the changing angle of attack are small which agrees with general predictions. The lowest and highest values for C_L are respectively 1.189 (taken at $t = 3.64$ s, marked on the graphs) and 1.297 (taken at $t = 4.04$ s). The variation of C_D is found to be even lower. Although changes are slight, it can be noticed in Figure 3 that higher angles of attack cause the vortices to grow in size. This further lowers the pressure on the upper surface, contributing to higher lift and drag. Reference areas of $0.25 \times chord \times span$ were used to obtain the coefficient values.

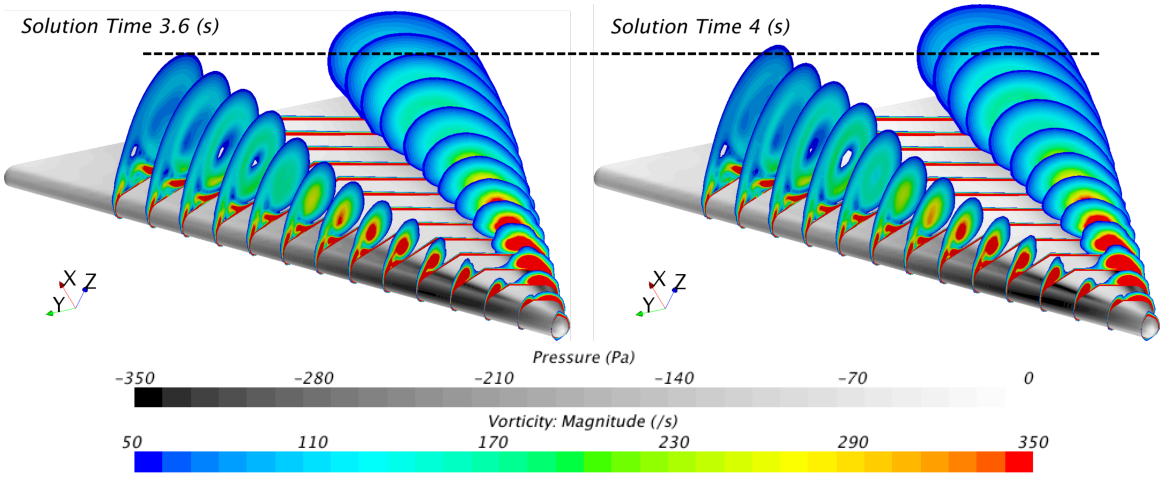

Figure 3: Vorticity and pressure on the delta wing corresponding to the lowest ($t = 3.6$ s) and highest ($t = 4.0$ s) coefficient values. Horizontal line is added to aid with comparison.

3.1 Lift and drag estimations and uncertainty

In order to conduct the uncertainty study, C_L and C_D values at $t = 3.64$ s are used. For grid and time step errors, an exponential function was used to find a best-fit line and estimate the ϕ_g and ϕ_t values, as seen in Figure 4.

For convergence uncertainty study, the values of coefficients at $t = 3.64$ s were compared with values at $t = 6.04$ s which also lie at the local minimum (lowest angle of attack). The uncertainties were then calculated using $U_\phi = 1.25|\phi| + \sigma$. However, due to the limited

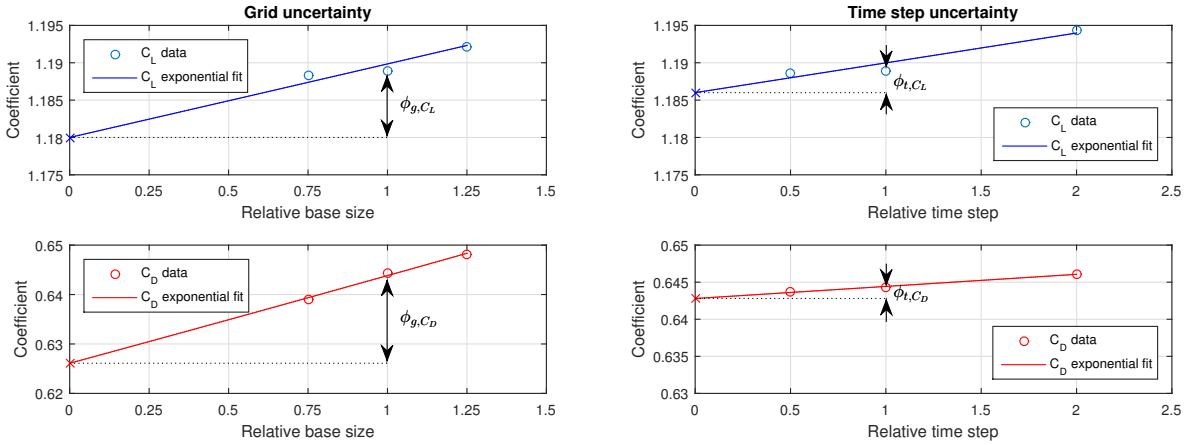

Figure 4: Grid and time uncertainty analysis.

number of simulation runs, standard deviation σ could not be determined precisely and was assumed to be 0. The results are summarised in Table 2. The errors due to round-off and

Coeff.	$\text{Value}_{\text{coarse}}$	$\text{Value}_{\text{base}}$	$\text{Value}_{\text{fine}}$	ϕ_{g}	ϕ_{t}	ϕ_{c}	$U_{\phi_{\text{g}}}$	$U_{\phi_{\text{t}}}$	$U_{\phi_{\text{c}}}$
C_L	1.192	**1.189**	1.888	0.0089	0.0029	0.0001	0.0111	0.0036	0.0001
C_D	0.648	**0.644**	0.639	0.0182	0.0015	0.0002	0.0228	0.0019	0.0003

Table 2: Coefficient values and uncertainty calculations.

other parameters of the numerics were assumed negligible. Using $U_{\phi_{\text{num}}} = \sqrt{U_{\phi_{\text{g}}}^2 + U_{\phi_{\text{t}}}^2} + U_{\phi_{\text{c}}}$ to calculate the final uncertainty, the estimations of hydrodynamic lift and drag coefficients are $C_L = 1.189 \pm 0.012$ and $C_D = 0.644 \pm 0.023$ at local minima and $C_L = 1.297 \pm 0.012$ and $C_D = 0.698 \pm 0.023$ at local maxima. The value of lift coefficient expected for Λ, α and Re used in this project can be read from the graph provided by Gursul [2] to be around $C_L^{\text{exp}} = 1.36$. This lies within an 8% error of the average value obtained for C_L, and hence, confirms that the estimation can be considered accurate.

3.2 Vortex breakdown and reattachment

Further justification of the accuracy of the simulation can be provided by comparing the vortex breakdown and reattachment behaviour of the flow. According to Gursul [3], for an angle of attack of $\alpha = 30°$ and wing sweep of $\Lambda = 64.84°$, a vortex breakdown and no reattachment close to the midplane of the wing should be expected. Such behaviour was observed and is shown in Figure 5. The velocity in the primary vortex core is observed to

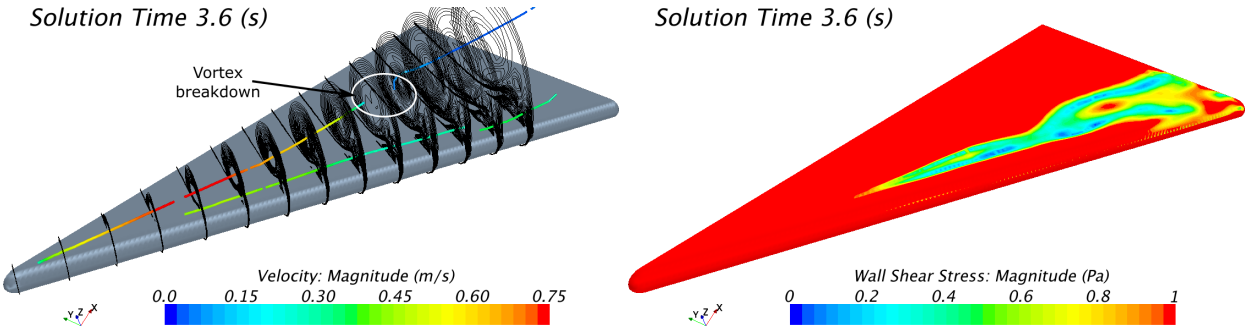

Figure 5: Vortex breakdown and wall shear stress plots.

suddenly decrease which causes the flow downstream to become wake-like. Such transition happens between $x = 0.7c$ and $x = 0.8c$ as measured from the apex of the wing. It also occurs at all variations of α from 28.7° to 31.3°. Moreover, since wall shear stress magnitude is found to be non-zero close to the midplane of the wing, it can be concluded that reattachment in that region does not occur. This agrees with the graph provided by Gursul [3].

3.3 Limitations and suggested improvements

If more time was available, volume of fluid (VOF) method would be used to model the free surface and waves. This would be done to verify that the theoretical velocity profile used in the simulations agrees with velocity field just below the free surface when modelled with VOF. No periodic vortex shedding was observed in the low time step simulation and this aspect of the flow could have been investigated further. According to Gordnier [1], this effect could change the lift coefficient by about 2.5%. In order to capture the shedding, grid would be further refined in the suitable region and time step reduced. Moreover, if more time or computational power was available, the simulations would be repeated to obtain the value of the standard deviation. By assuming $\sigma = 0$, the uncertainty calculated is underestimated. Lastly, more research would be done on the turbulence intensity and turbulence length scale values appropriate to the problem. It was difficult to estimate those properties precisely basing on the available literature. A laminar physics model would also be applied to run the simulations and compare the results. This would be motivated by the fact that, although reattachment points were present near the vortices, a high-turbulence shear layer reattachment zone was not observed close to the midplane of the wing.

4 Conclusions

The flow field around a submerged delta wing was analysed. Vortical flow structures were found on the suction side of the hydrofoil and they were identified to be the reason for the wing's ability to generate lift at an angle of attack of $\alpha = 30°$. As expected, the variations of forces with α were found to be low. Moreover, a vortex breakdown was observed to occur at around $0.75c$ from the apex of the wing. Also, no reattachment close to the midplane of the wing was present. Those results agreed with the graph provided by Gursul [3]. The final values for the coefficients of lift and drag at local minima were calculated to be $C_L = 1.189 \pm 0.012$ and $C_D = 0.644 \pm 0.023$.

5 References

[1] R. E. Gordnier and M. R. Visbal, "Unsteady vortex structure over a delta wing," *Journal of Aircraft*, vol. 31, no. 1, pp. 243–248, jan 1994.

[2] I. Gursul, R. Gordnier, and M. Visbal, "Unsteady aerodynamics of nonslender delta wings," *Progress in Aerospace Sciences*, vol. 41, no. 7, pp. 515–557, oct 2005.

[3] I. Gursul, Z. Wang, and E. Vardaki, "Review of flow control mechanisms of leading-edge vortices," *Progress in Aerospace Sciences*, vol. 43, no. 7-8, pp. 246–270, oct 2007.

[4] S. Collie, M. Gerritsen, and P. Jackson, "Performance of two-equation turbulence models for flat plate flows with leading edge bubbles," *Journal of Fluids Engineering*, vol. 130, no. 2, p. 021201, 2008.